

## Membrane potential of bipolar membranes

P. Ramírez<sup>a</sup>, S. Mafé<sup>b,\*</sup>, J.A. Manzanares<sup>b</sup>, J. Pellicer<sup>b</sup>

<sup>a</sup> *Departamento de Ciencias Experimentales, Universidad "Jaume I", Apdo 224, E-12080 Castellón, Spain*

<sup>b</sup> *Departamento de Termodinámica, Facultad de Física, Universidad de Valencia, E-46100 Burjassot, Spain*

Received 6 June 1995; in revised form 25 September 1995

### Abstract

The membrane potential of a bipolar membrane composed of a cation-exchange layer in series with an anion-exchange layer is analyzed theoretically and experimentally. The theoretical approach is based on an extension of the Nernst–Planck equations of monopolar charged membranes to the case of the two ion-exchange layers in series and the diffusion boundary layers adjacent to the bipolar membrane. The experimental results concern the transient behavior, stirring effects and concentration dependence of the membrane potential, and can be explained by means of the above theoretical approach. It is shown that membrane potential measurements can contribute significantly to a better electrochemical characterization of bipolar membranes.

*Keywords:* Membrane potential; Bipolar membrane; Cation exchange; Anion exchange

### 1. Introduction

A bipolar membrane (BM) consists of a cation-exchange layer in series with an anion-exchange layer. BM systems were considered in the past as simple models for biological membranes showing current rectification [1,2]. The first systematic studies on synthetic BMs were carried out by Frilette [3], Lovrecek et al. [4], and de Kőrös and Zeigerson [5]. More recently, BMs have been employed together with monolayer ion-exchange membranes to produce acid and alkali from salt and water by electrodialysis [6–9]. The electric field-enhanced water dissociation ("water splitting") occurring at the BM junction is the central problem in this case [10–18].

Since the main interest of BMs concerns their current rectification and water splitting properties, most theoretical and experimental studies have considered almost exclusively the phenomena associated with the passage of an electric current through the membrane [1–18] and, in particular, the current–voltage curves. However, open-circuit phenomena such as the membrane potential are often used to obtain valuable information on the selectivity of monopolar ion-exchange membranes [19,20], and could also contribute to a better electrochemical characterization of BMs. Though some model calculations have been pre-

sented previously [21,22], an experimental study devoted to the membrane potential of modern BMs seems to be lacking in the literature. Frilette [3] reported that "attempts to obtain a potential for a bipolar membrane in a concentration cell utilizing calomel electrodes and solution strengths varying from 0.01 to 0.3 M NaCl gave very erratic, irreproducible results, with large drifts of the readings." This is in marked contrast to the case of monopolar membranes, where membrane potential measurements give almost invariably steady-state values with good reproducibility [19,23–28].

We propose here to study theoretically and experimentally the membrane potential of a BM. The comparison of theory with experiments gives more insight into the membrane characteristics, and shows that a model based on the Nernst–Planck equations can explain the observed experimental trends. This model is basically an extension of the Teorell–Meyer–Sievers [19,20] theory of monopolar membranes to the case of the membrane system formed by the BM and the two diffusion boundary layers (DBLs) flanking it. The structure of this article is as follows. Firstly, we give a brief account of the theory and show some model calculations corresponding to different values of the membrane fixed charge concentrations, ionic diffusion coefficients and ion-exchange layer thicknesses. Then, we present the experimental results obtained for the membrane potential (transient behavior, reproducibility, stirring effects, etc.) over a broad range of concentration values and

\* Corresponding author.

concentration ratios. Finally, we discuss the plausibility of the membrane parameters obtained from the comparison of theory with experiment.

## 2. Theory

The ionic transport through a BM under different conditions has been studied extensively in the literature [1–3,5,6,13–18]. Concerning the calculation of the membrane potential of a BM, Sonin and Grossman [21] proposed an approximate solution valid when the fixed charge concentration of the ion-exchange layers is much greater than the concentration of the bathing solutions. Higuchi and Nakagawa [22] solved the problem numerically, and presented some model calculations for the case of a weakly charged BM separating two concentrated solutions. Sokirko et al. [29] analyzed theoretically the current–voltage characteristics of a BM under forward and reverse bias conditions, removing most of the simplifying assumptions introduced in previous studies. Their treatment can be used as a starting point to obtain the membrane potential of a BM.

Fig. 1 shows the BM system under study schematically. The cation-exchange layer has a negative fixed charge concentration  $X_N$  and lies from  $x = -d_L$  to  $x = 0$ . The anion-exchange layer extends from  $x = 0$  to  $x = d_R$  and carries a positive fixed charge concentration  $X_P$ . Both  $X_N$  and  $X_P$  are supposed to be uniform in each layer. The BM separates two aqueous solutions of the same univalent electrolyte whose concentrations are  $c_L$  in the left compartment and  $c_R$  in the right compartment.  $c_{iK}$  stands for the concentration of the  $i$ th ionic species in region  $K$  ( $i = 1$  for the cation,  $i = 2$  for the anion,  $K = N$  for the layer with negatively charged groups, and  $K = P$  for the layer with positively charged groups). The whole system is assumed to be isothermal, free from convective movements and chemical reactions, and at steady-state. It is necessary to incorporate two DBLs of thickness  $\delta$  adjacent to the membrane|solution interfaces: the existence of partial diffusion control by the DBLs is quite usual when an ion-exchange membrane is employed in a concentration cell [19]. This fact makes the theoretical analysis a little more

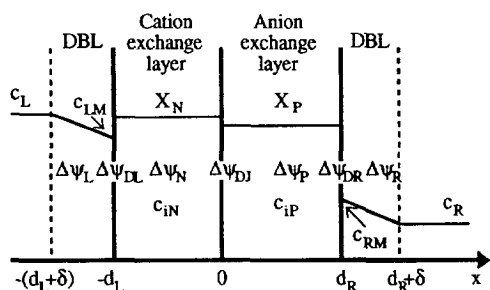


Fig. 1. Schematic view of the bipolar membrane system. We have incorporated two diffusion boundary layers (DBLs) adjacent to the membrane|solution interfaces.

involved [30]. Ideal Donnan equilibrium relationships [20] are assumed at the membrane|solution interfaces.

When no electric current passes through the BM, the ion fluxes  $J_i$  satisfy the equation

$$J_1 = J_2 \equiv J_s \quad (1)$$

where  $J_s$  is the salt flux through the membrane. The membrane potential can be computed as (see Fig. 1)

$$\begin{aligned} \Delta\phi_M &\equiv \phi(-d_L - \delta) - \phi(d_R + \delta) \\ &= \frac{RT}{F} (\Delta\psi_L + \Delta\psi_{DL} + \Delta\psi_N \\ &\quad + \Delta\psi_{DJ} + \Delta\psi_P + \Delta\psi_{DR} + \Delta\psi_R) \end{aligned} \quad (2)$$

where  $\Delta\psi_{DL}$ ,  $\Delta\psi_{DJ}$ , and  $\Delta\psi_{DR}$  are the dimensionless Donnan potentials at the interfaces  $x = -d_L$ ,  $x = 0$  and  $x = d_R$ , respectively, and  $\Delta\psi_L$ ,  $\Delta\psi_R$ ,  $\Delta\psi_N$ , and  $\Delta\psi_P$  are the dimensionless diffusion potentials in the bulk of the left and right DBL and in the ion-exchange layers N and P respectively. All electric potential differences are computed as left potential less right potential. Note that this is the opposite convention to that currently accepted for the e.m.f. and we have introduced it here only for the sake of consistency with previous studies [15,16,21,29]. In Eq. (2),  $R$  is the gas constant,  $T$  is the thermodynamic temperature, and  $F$  is the Faraday constant. Note that Eq. (2) contains seven terms instead of the three (two interfacial Donnan potentials plus the membrane diffusion potential) characteristic of monopolar membranes [19,23] because of the two ion-exchange layers of the BM and the partial diffusion control exerted by the DBLs.

Following Sokirko et al. [29], the individual potential drops in Eq. (2) can be written in terms of dimensionless variables as follows (see Fig. 1):

$$\Delta\psi_L = \tau_B \ln \frac{v_L}{v_{LM}} \quad (3)$$

$$\Delta\psi_{DL} = \ln \frac{v_N(-d_L) + 1}{v_{LM}} \quad (4)$$

$$\Delta\psi_N = \tau_N \ln \frac{v_N(-d_L) - \tau_N}{v_N(0) - \tau_N} \quad (5)$$

$$\Delta\psi_{DJ} = \ln \frac{[v_P(0) + 1] X_P}{[v_N(0) - 1] X_N} \quad (6)$$

$$\Delta\psi_P = \tau_P \ln \frac{v_P(0) + \tau_P}{v_P(d_R) + \tau_P} \quad (7)$$

$$\Delta\psi_{DR} = \ln \frac{v_{RM}}{v_P(d_R) - 1} \quad (8)$$

$$\Delta\psi_R = \tau_B \ln \frac{v_{RM}}{v_R} \quad (9)$$

where

$$v_K(x) \equiv \frac{c_{1K}(x) + c_{2K}(x)}{X_K}, \quad K = N, P \quad (10)$$

$$v_{LM} \equiv \frac{2c_{LM}}{X_N} \quad (11)$$

$$v_{RM} \equiv \frac{2c_{RM}}{X_P} \quad (12)$$

$$v_L \equiv \frac{2c_L}{X_N} \quad (13)$$

$$v_R \equiv \frac{2c_R}{X_P} \quad (14)$$

and

$$\tau_K \equiv \frac{D_{2K} - D_{1K}}{D_{2K} + D_{1K}} \quad K = N, P, B \quad (15)$$

Note that  $c_{LM}$  and  $c_{RM}$  are the salt concentrations in the solution side of the membrane|solution interfaces (see Fig. 1). In Eq. (15),  $D_{iK}$  ( $K = N, P$ ) stands for the diffusion coefficient of the  $i$ th species in the region  $K$ , and  $D_{iB}$  for the diffusion coefficient of species  $i$  in the DBLs. Application of the Donnan equilibrium conditions [20,31] to the interfaces  $x = -d_L$ ,  $x = d_R$  and  $x = 0$  yields

$$v_N(-d_L) = [1 + v_{LM}^2]^{1/2} \quad (16)$$

$$v_P(d_R) = [1 + v_{RM}^2]^{1/2} \quad (17)$$

$$v_P^{(0)} = \left\{ 1 + (X_N/X_P)^2 [v_N^2(0) - 1] \right\}^{1/2} \quad (18)$$

Consider the Nernst–Planck flux equations in the dilute solution form [23,31]. Integration of these equations in the DBLs and in regions N and P gives

$$v_{LM} = v_L - \frac{2\delta}{D_B X_N} J_s \quad (19)$$

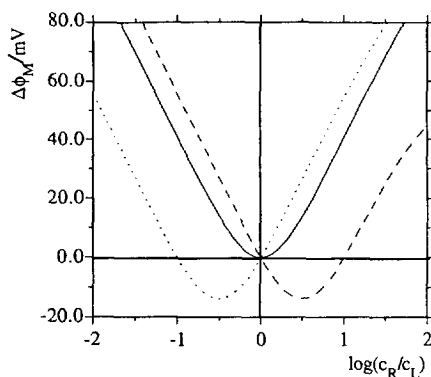


Fig. 2. Membrane potential  $\Delta\phi_M$  vs.  $\log(c_R/c_L)$  for the ratios  $X_N/X_P = 0.1$  (-----),  $X_N/X_P = 1$  (—), and  $X_N/X_P = 10$  (·····). In all cases  $\delta = 0 \mu\text{m}$ ,  $d_L = d_R = 50 \mu\text{m}$ ,  $D_{iK} = 10^{-10} \text{ m}^2 \text{ s}^{-1}$  ( $i = 1, 2$ ;  $K = N, P$ ) and  $c_L = 0.01 \text{ M}$ .

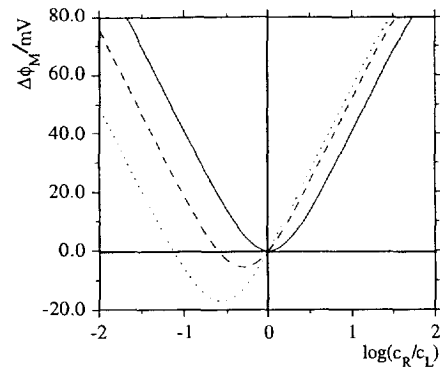


Fig. 3. Membrane potential  $\Delta\phi_M$  vs.  $\log(c_R/c_L)$  for the ratios  $D_{2N}/D_{1N} = 2$  and  $D_{2P}/D_{1P} = 1$  (-----),  $D_{2N}/D_{1N} = D_{2P}/D_{1P} = 1$  (—), and  $D_{2N}/D_{1N} = 2$  and  $D_{2P}/D_{1P} = 0.1$  (·····). In all cases  $\delta = 0 \mu\text{m}$ ,  $d_L = d_R = 50 \mu\text{m}$ ,  $X_N = X_P = 1 \text{ M}$ ,  $D_{2N} = D_{1P} = 10^{-10} \text{ m}^2 \text{ s}^{-1}$  and  $c_L = 0.01 \text{ M}$ .

$$v_N(0) = v_N(-d_L) + \Delta\psi_N - \frac{2d_L}{D_N X_N} J_s \quad (20)$$

$$v_P(0) = v_P(d_R) + \Delta\psi_P \frac{2d_R}{D_P X_P} J_s \quad (21)$$

$$v_{RM} = v_R + \frac{2d}{D_B X_P} J_s \quad (22)$$

where

$$D_K \equiv \frac{2D_{1K} D_{2K}}{D_{1K} + D_{2K}} \quad K = N, P, B \quad (23)$$

is the salt diffusion coefficient in region  $K$ .

Eqs. (18)–(22) allow for the calculation of the five unknowns  $v_{LM}$ ,  $v_{RM}$ ,  $v_N(0)$ ,  $v_P(0)$  and  $J_s$ . Note that, since  $v_{LM}$ ,  $v_{RM}$  and  $J_s$  can be written in terms of  $v_N(0)$  and  $v_P(0)$ , only two of these unknowns need to be solved numerically. Finally, substitution of  $v_{LM}$ ,  $v_{RM}$ ,  $v_N(0)$ ,  $v_P(0)$  and  $J_s$  into Eqs. (3)–(9) gives the membrane potential in Eq. (2) as a function of the characteristic parameters of the two layers.

The behavior of the above system of equations can be understood with the help of some model calculations. As previously reported in the literature [22], we see from Figs. 2–4 that the  $\Delta\phi_M$  vs.  $\log(c_R/c_L)$  curves are quite sensitive to the ratios  $X_N/X_P$  and  $d_L/d_R$ , and to the values of the diffusion coefficients  $D_{iK}$ . In all these figures we have fixed  $\delta = 0 \mu\text{m}$ ,  $c_L = 0.01 \text{ M}$  and  $D_{1P} = D_{2N} = 10^{-10} \text{ m}^2 \text{ s}^{-1}$ .

In Fig. 2 we have taken  $d_L = d_R = 50 \mu\text{m}$ ,  $D_{1N} = D_{2P} = 10^{-10} \text{ m}^2 \text{ s}^{-1}$ , and varied  $X_N$  and  $X_P$  in the form: (i)  $X_N = 0.1 \text{ M}$ ,  $X_P = 1 \text{ M}$  (dashed line); (ii)  $X_N = X_P = 1 \text{ M}$  (continuous line); and (iii)  $X_N = 1 \text{ M}$ ,  $X_P = 0.1 \text{ M}$  (dotted line). In Fig. 3 we have taken  $d_L = d_R = 50 \mu\text{m}$ ,  $X_N = X_P = 1 \text{ M}$  and varied  $D_{2N}/D_{1N}$  and  $D_{2P}/D_{1P}$  in the form: (i)  $D_{2N}/D_{1N} = 2$  and  $D_{2P}/D_{1P} = 1$  (dashed line); (ii)  $D_{2N}/D_{1N} = D_{2P}/D_{1P} = 1$  (continuous line); and (iii)

$D_{2N}/D_{1N} = 2$  and  $D_{2P}/D_{1P} = 0.1$  (dotted line). In Fig. 4 we have taken  $D_{1N} = D_{2P} = 10^{-10} \text{ m}^2 \text{ s}^{-1}$ ,  $X_N = X_P = 1 \text{ M}$  and varied  $d_L$  and  $d_R$  in the form: (i)  $d_L = 10 \text{ }\mu\text{m}$  and  $d_R = 100 \text{ }\mu\text{m}$  (dashed line); (ii)  $d_L = d_R = 100 \text{ }\mu\text{m}$  (continuous line); and (iii)  $d_L = 100 \text{ }\mu\text{m}$  and  $d_R = 10 \text{ }\mu\text{m}$  (dotted line).

The position of the minima in these curves is determined by the symmetry properties of the BM. In Fig. 2, the symmetric case  $X_N/X_P = 1$  gives a minimum for  $c_R = c_L$ , while the minimum is reached when  $c_R < c_L$  ( $c_R > c_L$ ) for  $X_N > X_P$  ( $X_N < X_P$ ). In Fig. 3, deviations from symmetry in the ratios  $D_{2N}/D_{1N}$  and  $D_{2P}/D_{1P}$  also shift the position of the minima. Finally, the symmetric case  $d_L = d_R$  in Fig. 4 gives a minimum for  $c_R = c_L$ , while the minimum is shifted to  $c_R < c_L$  ( $c_R > c_L$ ) when  $d_L > d_R$  ( $d_L < d_R$ ).

In the case  $c_{L,R} \ll X_{N,P}$ , and ignoring the diffusional contribution, the membrane potential of the bipolar membrane can be approximated by

$$\Delta\phi_M = \frac{RT}{F} \ln \frac{c_R d_L X_N / c_L D_{2N} + c_L d_R X_P / c_R D_{1P}}{d_L X_N / D_{2N} + d_R X_P / D_{1P}} \quad (24)$$

which can be seen as an extension of the equation derived first in Sonin and Grossman's model [21]. The membrane potential in Eq. (24) attains a minimum when

$$c_R / c_L = (d_R X_P D_{2N} / d_L X_N D_{1P})^{1/2} \quad (25)$$

The minima given by Eqs. (24), (25) agree with those in Figs. 2 and 4. The existence of the minimum can be explained from the relative values of the interfacial potential drops. In the symmetric case  $X_N = X_P = X$  in Fig. 2, these potential drops are

$$\Delta\psi_{DL} = \ln(X/c_L) \quad (26)$$

$$\Delta\psi_{DJ} = \ln \frac{c_L^2 + c_R^2}{2X^2} \quad (27)$$

and

$$\Delta\psi_{DR} = \ln(X/c_R) \quad (28)$$

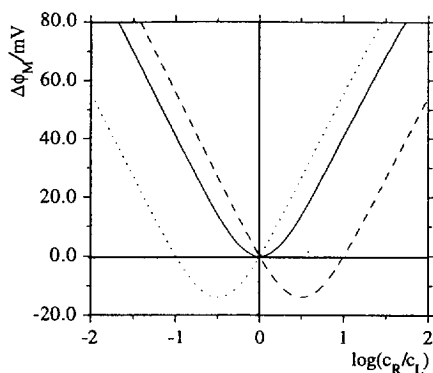


Fig. 4. Membrane potential  $\Delta\phi_M$  vs.  $\log(c_R/c_L)$  for the ratios  $d_L/d_R = 0.1$  (-----),  $d_L/d_R = 1$  (—), and  $d_L/d_R = 10$  (.....). In all cases  $\delta = 0 \text{ }\mu\text{m}$ ,  $X_N = X_P = 1 \text{ M}$ ,  $D_{iK} = 10^{-10} \text{ m}^2 \text{ s}^{-1}$  ( $i = 1, 2, K = N, P$ ) and  $c_L = 0.01 \text{ M}$ .

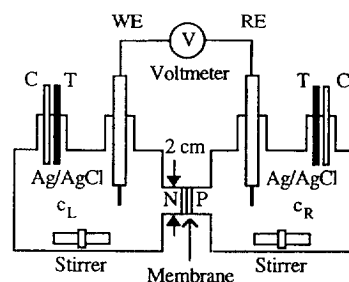


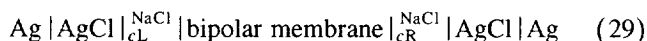
Fig. 5. Sketch of the experimental setup. WE and RE are the working and reference electrodes respectively. T and C are the temperature and conductivity probes.

The potential drops in Eqs. (26) and (28) are always positive. The potential drop  $\Delta\psi_{DJ}$  is always negative, but remains lower than the sum  $\Delta\psi_{DL} + \Delta\psi_{DR}$ . As the total membrane potential should be zero at  $c_R = c_L$ , it is clear from Eqs. (26)–(28) that a minimum must appear at this point. Although the analysis of the asymmetric cases is more cumbersome, qualitative plots of the electric potential profiles through the membrane interfaces can readily justify the position of the minimum given by Eq. (25).

From the above results, we conclude that it is possible to deduce important information on the BM symmetry from the membrane potential data. The symmetry of the two ion-exchange layers seems to be important for improving the efficiency of the water splitting phenomenon [13,29,32].

### 3. Experimental

The experimental setup used to measure the membrane potential of the BM is shown schematically in Fig. 5. The exposed area of the BM was  $3.1 \text{ cm}^2$ . The whole membrane cell can be represented as



The solutions were stirred vigorously by means of magnetic stirrers. The NaCl concentration  $c_L$  in the left compartment was taken as the reference concentration and kept constant during each experimental series for the different values considered for the ratio  $c_R/c_L$ . Two series of measurements,  $c_L = 10^{-2} \text{ M}$  and  $c_L = 1 \text{ M}$ , were carried out. The e.m.f. of the cell was measured by inserting directly into the solutions a pair of Ag|AgCl electrodes connected to a high impedance voltmeter (a micro pH meter Crison 2002 with an input impedance of  $10^{14} \text{ }\Omega$ ).

Each measurement gives necessarily the emf of the whole cell from which the two electrode potentials must be subtracted in order to obtain the membrane potential [19,33,34]. The electrode potential difference was calculated in terms of the activity of the chloride ion because of the relatively high concentrations of some of the solutions employed. An assumption about the single-ion activity coefficient  $\gamma_{\text{Cl}^-}$  was then needed. We assumed [19] that

$\gamma_{\text{Cl}^-} \approx \gamma_{\text{NaCl}}$ , where  $\gamma_{\text{NaCl}}$  is the activity coefficient of the salt. The activity coefficients were obtained from tabulated data [35,36]. The correction for the electrode potential difference could be avoided by using calomel electrodes instead of Ag|AgCl electrodes [19,24,37]. However, some uncertainties concerning the diffusion potentials at the KCl bridges would appear in this case [19,38].

The separation of the e.m.f. of the cell shown in Eq. (29) into the “single” potential differences of Eq. (2) plus the electrode potential difference might be questionable in the sense that these individual differences cannot be obtained by direct measurements. Still, the introduction of the single potential differences gives a satisfactory intuitive view of the charge separation which occurs through the system, and has therefore been extensively used in the literature [19,20,23].

The BM studied was a membrane designed and developed at the Fraunhofer-Institut für Grenzflächen- und Bioverfahrenstechnik, FhIGB, (Stuttgart, Germany). The anion-exchange layer was prepared by incorporating a quaternary ammonium ion into a polysulfone matrix. The cation-exchange layer was a cross-linked sulfonated polyetherketone with the strongly acid sulfonic acid group as fixed charge. A very thin intermediate layer (about 10 nm thick) of an insoluble polyelectrolyte complex was inserted between the two layers. This layer promotes high water dissociation rates during bipolar electro dialysis [39] in the high current regime, but is expected to produce negligible effects for the case of the membrane potential measurements because of its small thickness. Particular details about the membrane preparation can be found in Refs. [39] and [40]. Solutions were prepared from Panreac (Montplet & Esteban, Barcelona, Spain) pro analysis grade chemicals (without further purification) and distilled water. The pH of the solutions was that of distilled water.

The BM under study was equilibrated with the reference solution of NaCl during 24 h before each run. The conductivity of the solutions in the adjacent cells was periodically measured in order to detect any change in

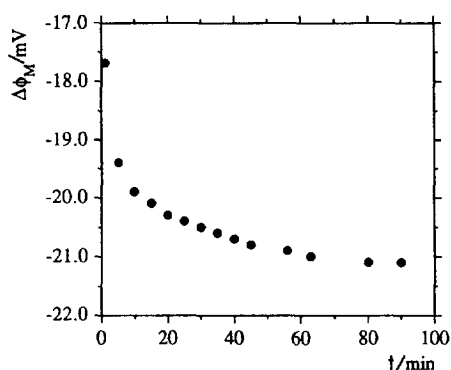


Fig. 6. Transient behavior for the membrane potential of the BM in the case of no stirring. The concentrations were  $c_L = 0.01$  M and  $c_R = 5 \times 10^{-3}$  M.

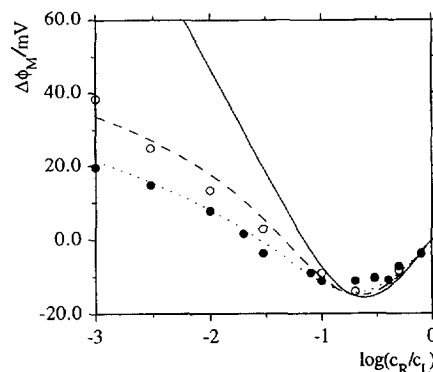


Fig. 7. Membrane potential  $\Delta\phi_M$  vs.  $\log(c_R/c_L)$  for  $c_L = 1$  M in the cases of no stirring (●) and stirring (○). The theoretical curves correspond to  $\delta = 0$   $\mu\text{m}$  (—),  $\delta = 100$   $\mu\text{m}$  (---), and  $\delta = 200$   $\mu\text{m}$  (.....).

their concentration. The experimental results were taken at room temperature (25°C).

#### 4. Results and discussion

Fig. 6 shows a typical transient behavior for the membrane potential of the BM. The steady-state was reached within several tens of minutes (without any stirring). All series of measurements showed that the greater the deviations of  $c_R/c_L$  from unity, the longer the time to attain the steady-state. It was also found that stirring of the solutions reduced this time down to several minutes. Therefore, the transient behavior depends not only on the initial state of the membrane, but also on the state of the adjacent DBLs [19]. Still, if we accept that the transient time for the membrane potential is at least of the order of the diffusional relaxation time within the membrane,  $\tau = (d_L + d_R)^2/D_{\text{BM}}$ , then a typical diffusion coefficient  $D_{\text{BM}}$  would be of the order of  $10^{-10}$   $\text{m}^2 \text{s}^{-1}$ , since  $(d_L + d_R)$  is of the order of  $10^{-4}$  m [39,40].

The asymmetric structure of the BM gave very different values of the membrane potential when, for a fixed value of  $c_L/c_R$ , the positions of the two ion-exchange layers of the membrane were interchanged. Thus, in the case  $c_R = 0.01$  M and  $c_L = 1$  M, we obtained  $\Delta\phi_M = 8$  mV when the layer N was facing the left compartment and  $\Delta\phi_M = -55$  mV when the layer N was facing the right compartment.

Fig. 7 shows the plot of  $\Delta\phi_M$  vs.  $\log(c_R/c_L)$  for  $c_L = 1$  M. The cases of stirring (open circles) and no stirring (full circles) of the bathing solutions are shown. The continuous line corresponds to the theoretical predictions for  $\delta = 0$   $\mu\text{m}$ . These theoretical predictions follow the experimental data only when  $c_R$  is close to  $c_L$ . The theory fails in the region  $c_R \ll c_L$ . Since the experimental data show that the effects of stirring are more noticeable in this region, the disagreement between theory and experi-

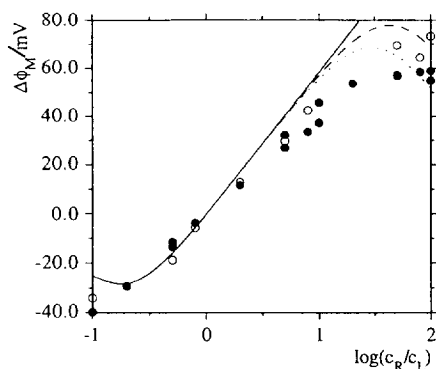


Fig. 8. Membrane potential  $\Delta\phi_M$  vs.  $\log(c_R/c_L)$  for  $c_L = 0.01$  M in the cases of no stirring ( $\bullet$ ) and stirring ( $\circ$ ). The theoretical curves correspond to  $\delta = 0$   $\mu\text{m}$  (—),  $\delta = 100$   $\mu\text{m}$  (-----), and  $\delta = 200$   $\mu\text{m}$  (.....).

ment can be due to the existence of DBLs. Indeed, introducing  $\delta = 100$   $\mu\text{m}$  (dashed line) and  $\delta = 200$   $\mu\text{m}$  (dotted line), which are two typical values for the DBL thickness observed in ion-exchange membranes [19,33,41,42], and taking for  $D_B$  the salt diffusion coefficient value at infinite dilution, a good agreement between theory and experiment is achieved. We see from Fig. 7 that a vigorous stirring of the bathing solutions diminishes the thickness of the DBL, but it does not eliminate completely its effects. We have used the membrane parameters  $X_N = 2$  M,  $X_P = 1$  M,  $d_L = 70$   $\mu\text{m}$  and  $d_R = 20$   $\mu\text{m}$ , which are very close to the values found previously by the designers of the BM using independent methods [39]. The best fit was obtained for the diffusion coefficients  $D_{1N} = 10^{-10}$   $\text{m}^2 \text{s}^{-1}$ ,  $D_{2N} = 10^{-10}$   $\text{m}^2 \text{s}^{-1}$ ,  $D_{1P} = 5 \times 10^{-10}$   $\text{m}^2 \text{s}^{-1}$ , and  $D_{2P} = 10^{-10}$   $\text{m}^2 \text{s}^{-1}$ . Ionic diffusion coefficients of the same order of magnitude were found in the study of the current–voltage curves of this BM under direct and reverse polarization [16]. Ionic diffusion coefficients are typically one order of magnitude smaller in ion-exchange membranes than in free solution [19].

Fig. 8 presents the plot  $\Delta\phi_M$  vs.  $\log(c_R/c_L)$  for  $c_L = 0.01$  M. The cases of stirring (open circles) and no stirring (full circles) of the bathing solutions are also shown. Again, the continuous line corresponds to the theoretical predictions with  $\delta = 0$   $\mu\text{m}$ , the dashed line to  $\delta = 100$   $\mu\text{m}$ , and the dotted line to  $\delta = 200$   $\mu\text{m}$ . The theory with  $\delta = 0$   $\mu\text{m}$  fails now in the region  $c_L \ll c_R$ , which corresponds to high concentration gradients. This is just the same trend observed in Fig. 7. (Note that the higher the concentration gradient, the greater the salt flux through the membrane, and the more important the DBL effects.) Also, as we can see from Fig. 8, the reproducibility of the membrane potential measurements is quite good (better than 5% in most of the cases). The theoretical curves in Fig. 8 were calculated using the same membrane parameters as in Fig. 7. Since the ionic diffusion coefficients in free solution depend on concentration, it is likely that the agreement between theory and experiment in Fig. 8 could

still be improved by changing slightly the values found for the  $D_{iK}$  in Fig. 7. However, these coefficients are not only properties of a particular ion [31], but depend also on the characteristics of the ion-exchange layers [19]. In view of these uncertainties, and in order not to increase the number of free parameters in the model, we did not attempt to change the values of the  $D_{iK}$  in Fig. 7.

In conclusion, we have shown that the study of membrane potential can also contribute to the electrochemical characterization of BMs. We have seen that a simple model based on the Nernst–Planck equations can explain the experimental trends observed for the membrane potential of a BM under a broad range of concentration ratios. In this context, it should be mentioned that the results obtained from the Nernst–Planck equations often give good first approximations to the ion transport properties of monopolar membranes [31], though it is invariably the case that further refinements are still necessary for quantitative purposes. In our case, the omission of cross-terms and activity coefficients in the above equations [31,43] may be questionable in the higher concentration range, and thus the membrane parameters reported here might have some uncertainties. Still, it is reassuring that the values of these parameters are close to those previously found [15,16,39, 40] by using independent experimental methods, and this should be correct to within (at least) an order of magnitude.

#### Acknowledgements

We thank Antonio Guirao (Dpto. de Física, Univ. de Murcia, Spain) and Dr. Vicente Compañ (Dpto. de Ciencias Experimentales, Univ. Jaume I de Castellón, Spain) for their helpful experimental assistance. The bipolar membranes were kindly supplied by Dr. Bernd Bauer (Gesellschaft für Umweltkompatible Proceßtechnik mbH, Saarbrücken, Germany). Financial support from the Plan Valenciano de Ciencia y Tecnología (Conselleria de Educación y Ciencia) under the “Grupos Emergentes” program is gratefully acknowledged.

#### References

- [1] A. Mauro, *Biophys. J.*, 2 (1962) 179.
- [2] H.G.L. Coster, *Biophys. J.*, 5 (1965) 669.
- [3] V.J. Filette, *J. Phys. Chem.*, 60 (1956) 435.
- [4] B. Lovrecek, V. Srb and B. Kunst, *Electrochim. Acta*, 12 (1967) 905.
- [5] F. de Kőrös and E. Zeigerson, *Isr. J. Chem.*, 9 (1971) 483.
- [6] B. Bauer, F.J. Gerner and H. Strathmann, *Desalination*, 68 (1988) 279.
- [7] F.P. Chlanda, Y.C. Chiao and K. Mani, in K.K. Sirkar and D.R. Lloyd (Eds.), *New Membrane Materials and Processes for Separation*, AIChE Symp. Ser., New York, 1988, Vol. 84.
- [8] Y.C. Chiao, F.P. Chlanda and K. Mani, *J. Membr. Sci.*, 61 (1991) 239.

- [9] K. Mani, *J. Membr. Sci.*, 58 (1991) 117.
- [10] R. Simons, *Nature*, 280 (1979) 824.
- [11] R. Simons, *Electrochim. Acta*, 29 (1984) 151.
- [12] R. Simons, *Electrochim. Acta*, 30 (1985) 275.
- [13] I.C. Bassignana and H. Reiss, *J. Membr. Sci.*, 15 (1983) 27.
- [14] V.I. Zabolotskii, N.V. Shel'deshov and N.P. Gnusin, *Russ. Chem. Rev.*, 57 (1988) 801.
- [15] P. Ramírez, H.J. Rapp, S. Reichle, H. Strathmann and S. Mafé, *J. Appl. Phys.*, 72 (1992) 259.
- [16] P. Ramírez, H.J. Rapp, S. Mafé and B. Bauer, *J. Electroanal. Chem.*, 375 (1994) 101.
- [17] R. El Moussaoui, G. Pourcelly, M. Maecck, H.D. Hurwitz and C. Gavach, *J. Membr. Sci.*, 90 (1994) 283.
- [18] N.T. Dang and D. Woermann, *Ber. Bunsenges. Phys. Chem.*, 97 (1993) 149.
- [19] F. Helfferich, *Ion Exchange*, McGraw-Hill, New York, 1962.
- [20] N. Lakshminarayanaiah, *Equations of Membrane Biophysics*, Academic Press, New York, 1984.
- [21] A.A. Sonin and G. Grossman, *J. Phys. Chem.*, 76 (1972) 3996.
- [22] A. Higuchi and T. Nakagawa, *J. Membr. Sci.*, 32 (1987) 267.
- [23] R.P. Buck, *CRC Crit. Rev. Anal. Chem.*, 5 (1976) 323.
- [24] W. Pusch, in E. Sélégny (Ed.), *Charged Gels and Membranes I*, D. Reidel, Dordrecht, 1976.
- [25] Y. Kimura, H.J. Lim and T. Iijima, *J. Membr. Sci.*, 18 (1984) 285.
- [26] A. Higuchi and T. Iijima, *J. Appl. Polym. Sci.*, 31 (1986) 419.
- [27] M. Cappadonia, K. Doblhofer and D. Woermann, *J. Colloid. Interface Sci.*, 143 (1991) 222.
- [28] K. Asaka, *J. Membr. Sci.*, 52 (1990) 57.
- [29] A.V. Sokirko, P. Ramírez, J.A. Manzanares and S. Mafé, *Ber. Bunsenges. Phys. Chem.*, 97 (1993) 1040.
- [30] S. Mafé, V.M. Aguilera and J. Pellicer, *J. Membr. Sci.*, 36 (1988) 497.
- [31] R.P. Buck, *J. Membr. Sci.*, 17 (1984) 1.
- [32] P. Ramírez, J.A. Manzanares and S. Mafé, *Ber. Bunsenges. Phys. Chem.*, 95 (1991) 499.
- [33] E. Kumamoto, *J. Membr. Sci.*, 9 (1981) 43.
- [34] T.S. Sørensen and J.B. Jensen, *J. Non-Equilib. Thermodyn.*, 9 (1984) 1.
- [35] R.A. Robinson and R.H. Stokes, *Electrolyte Solutions*, Butterworths, London, 1959.
- [36] H.P. Bennetto and J.J. Spitzer, *J. Chem. Soc., Faraday Trans. I*, 1 (1977) 1066.
- [37] J. Benavente, *J. Non-Equilib. Thermodyn.*, 9 (1984) 217.
- [38] N.O. Østerberg, T.S. Sørensen and J.B. Jensen, *J. Electroanal. Chem.*, 119 (1981) 93.
- [39] H. Strathmann, B. Bauer and H.J. Rapp, *Chemtech*, June (1993) 17.
- [40] H. Strathmann, H.J. Rapp, B. Bauer and C.M. Bell, *Desalination*, 90 (1993) 303.
- [41] R.J. French, *Biophys. J.*, 18 (1977) 53.
- [42] A. Guirao, S. Mafé, J.A. Manzanares and J.A. Ibáñez, *J. Phys. Chem.*, 99 (1995) 3387.
- [43] D.G. Müller, *Disc. Faraday Soc.*, 64 (1978) 295.

#### Note added in proof

While this manuscript was in press, a study on the membrane potential of bipolar membranes appeared (M. Higa and A. Kira, *J. Phys. Chem.*, 99 (1995) 5089).